Supporting Information

Self-Powered Human-Health Monitoring through Aligned PVDF Nanofibers Interfaced Skin-Interactive Piezoelectric Sensor

Kuntal Maity,[a] Samiran Garain,[a,b,†] Karsten Henkel,[b,c] Dieter Schmeiβer,[b] Dipankar Mandal[a,d*]

[a]Organic Nano-Piezoelectric Device Laboratory, Department of Physics, Jadavpur University, Kolkata 700032, India

[b]Applied Physics and Sensor Technology, Brandenburg University of Technology Cottbus-Senftenberg, Konrad-Wachsmann-Allee 17, 03046 Cottbus, Germany

[c]Applied Physics and Semiconductor Spectroscopy, Brandenburg University of Technology Cottbus-Senftenberg, Konrad-Zuse-Straße 1, 03046 Cottbus, Germany

[d]Institute of Nano Science & Technology, Habitat Centre, Phase 10, Sector 64, Mohali 160062, India

† This author currently working as a Post-Doctoral Research Associate in Kyung Hee University, Yongin, Gyeonggi 17104 South Korea.

[*]Corresponding author:

E-mail addresses: *dipankar@phys.jdvu.ac.in*, *dmandal@inst.ac.in*

Note S1. Preparation of the PANI coated PVDF NFs mat.

The PANI coated PVDF NFs were prepared by two-step procedure. Firstly, the oxidant containing PVDF NFs mat was prepared by electrospinning technique (mentioned above) where 1 wt% $FeCl_3$, 6 H_2O was mixed into the PVDF solution in prior to electrospinning. Subsequently, the resulting solution was electrospun and collected the $FeCl_3$ containing PVDF NFs mat (yellowish color) upon the Al foil covered grounded collector. Secondly, PANI coated PVDF NFs mat was prepared through *in-situ* conversion of aniline monomer by VPP. At first, an aniline/HCl solution was prepared with a volume ratio of 1:10 under continuous stirring at 500 rpm for about 30 min in a 100 ml beaker. Then, 0.5 g APS was added into the solution and the stirring was kept for another 30 min. After that, the mixed solution was transferred into a container having a sample holder inside. The as-prepared $FeCl_3$/PVDF NF mats having an area of 4×2 cm^2 obtained by the electrospinning method was then placed upon this sample holder in the middle keeping a certain distance to the solution inside the container. After placing the NFs mat the whole container is sealed tightly and kept upon a hot plate at 180°C for about 6 h. Finally, the resulting PANI coated PVDF NFs mat (deep blackish color) was taken out from the container, washed continuously with deionized water and subsequently dried in air at room temperature.

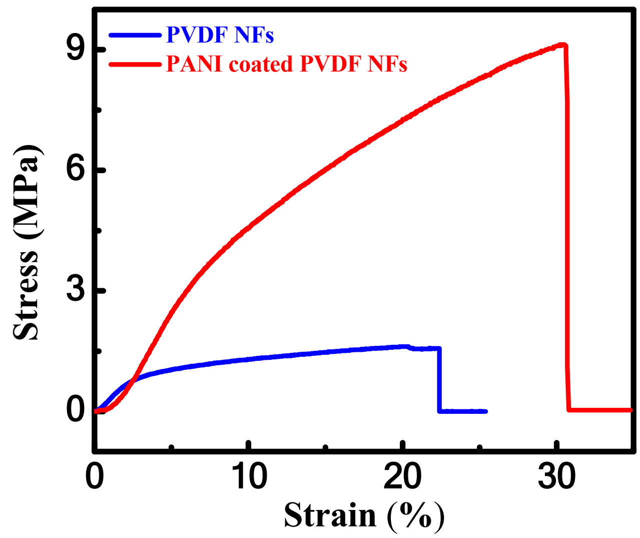

Figure S1. Mechanical properties (stress vs. strain curve) of PANI coated PVDF NFs mat and PVDF NFs mat.

Note S2. Mechanical properties of PANI-PVDF NFs mat and PVDF NFs mat.

In accordance with PANI coating, the mechanical characteristics of the PVDF NFs mats were checked before and after coating as these properties determine the long term performance of the device. Figure S1 presents the respective stress vs. strain curves which exhibits a higher tensile stress of PANI coated PVDF NFs than that of PVDF NFs mat. This result is attributed to the stress concentration caused by the coating of PANI network upon the PVDF NFs mat in comparison to the PVDF NFs mat during VPP. The PANI tied on the surface of PVDF NFs and enhances the mechanical stability. From the curve in Figure S1, the Young's modulus (Y) was calculated and values of 65 MPa and 9 MPa were obtained for the PANI-PVDF NFs mat and PVDF NFs mat, respectively. Therefore, the good mechanical property of the PANI-PVDF NFs mat discloses its potential application in POESS.

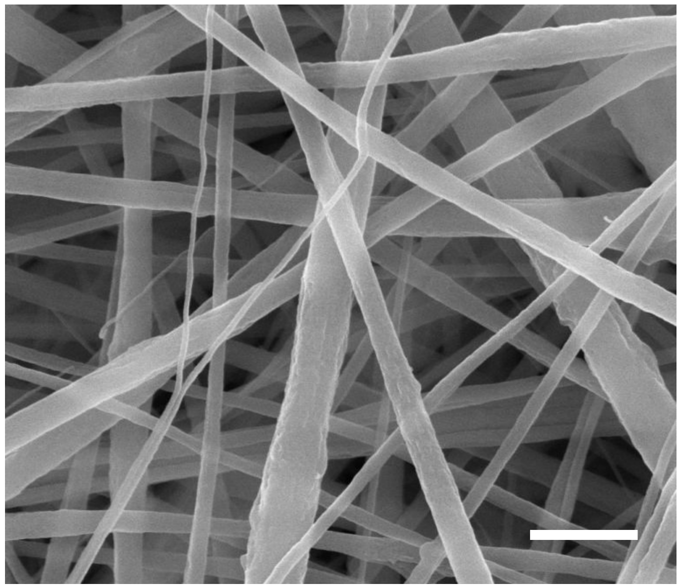

Figure S2. FE-SEM image of the randomly oriented PVDF NFs; the scale bar corresponds to 1 μm.

Note S3. Calculation of the degree of crystallinity.

The total degree of crystallinity (χ_{ct}) was calculated using the curve deconvolution technique as,

$$\chi_{ct} = \frac{\Sigma A_{cr}}{\Sigma A_{cr} + \Sigma A_{amr}} \times 100\% \tag{1}$$

where ΣA_{cr} and ΣA_{amr} are the summation of the integral areas of the crystalline peaks and the amorphous halo correspondingly. The degrees of β-crystallinity ($\chi_{c\beta}$) and α- crystallinity ($\chi_{c\alpha}$) was evaluated as:

$$\chi_{c\beta} = \chi_{ct} \times \frac{\Sigma A_{\beta}}{\Sigma A_{\beta} + \Sigma A_{\alpha}} \tag{2}$$

$$\chi_{c\alpha} = \chi_{ct} \times \frac{\Sigma A_{\alpha}}{\Sigma A_{\beta} + \Sigma A_{\alpha}} \tag{3}$$

where ΣA_{β} and ΣA_{α} are the summation of the integral areas of the β-phase peak and the α- phase peak, respectively.

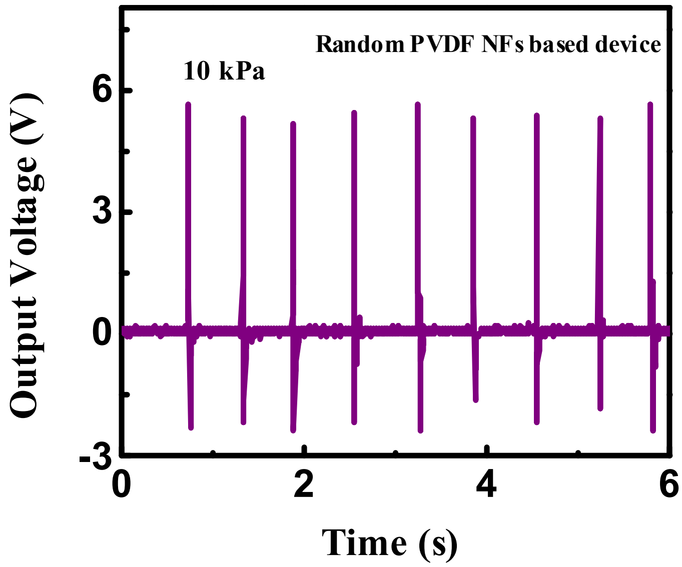

Figure S3. Open-circuit output voltage response (V_{oc}) of a control device based on randomly oriented PVDF NFs with PANI coated PVDF NFs mat as electrodes keeping the device dimensions and other conditions the same as in the device with aligned PVDF NFs (Figure 4a, main manuscript) under hand punching of 10 kPa pressure.

Table S1: Comparison of present state-of-the-art device performance of piezoelectric sensors in terms of nanofiber orientation. (t: thickness of the piezoelectric material, A: working area of the piezoelectric material, NF: not found)

Materials	Nanofiber Orientation Type	Device Details (dimension)	Applied Frequency, Force/Pressure	Output Voltage (V_{oc})	Output Current (I_{sc})	References
PVDF-$NaNbO_3$	Random	t = 162 µm , A= 6.3 cm^2	1 Hz, 0.2 MPa	3.4 V	4.4 µA	[S1]
PVDF-ZnO	Random	t= 120 µm, A= 4 cm^2	75 kHz	1.1 V	NF	[S2]
PVDF-Ce^{3+}/ Graphene	Random	t= NF, A=1200 mm^2	4 Hz, 8N	11 V	NF	[S3]
PVDF-MoS_2	Random	t= 150 µm, A= 93.5 cm^2	7 N	14 V	NF	[S4]
P(VDF-TrFE)	Aligned	t= 10-40 µm, A= 36 mm^2	2 Hz	1.5 V	40 nA	[S5]
PLZT	Aligned	NF	NF	5 V	42 nA	[S6]
P(VDF-TrFE)	Aligned	t= 0.4 cm, A= 16.2 cm^2	2 Hz, 2 kPa	5 V	875 nA	[S7]
PVDF	Aligned	t= 150 µm, A= 18 cm^2	10 kPa	10 V	6 µA/cm^2	This work

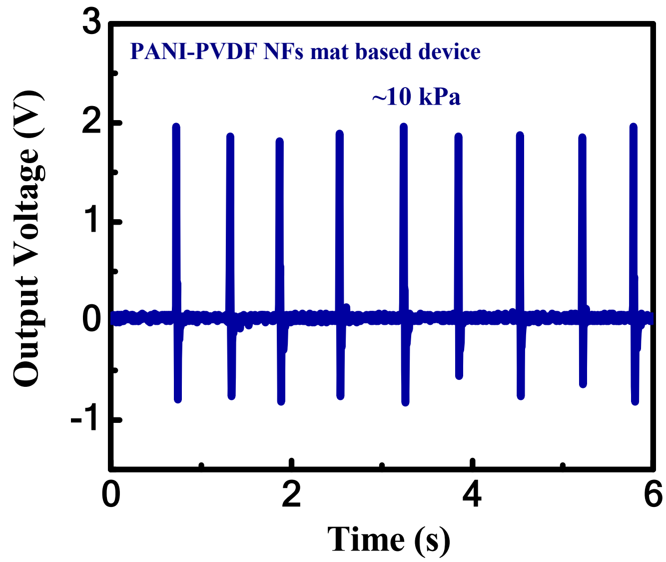

Figure S4. Open-circuit output voltage response (V_{oc}) of a device based on only PANI-PVDF NFs mat keeping device dimensions and other conditions the same as in the regular POESS device under hand punching of 10 kPa pressure.

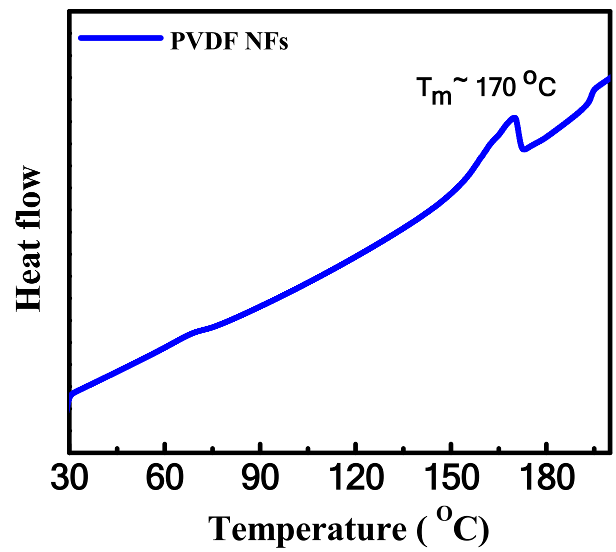

Figure S5. Differential Scanning Calorimetry **(**DSC) thermal study of PVDF NFs.

Note S4. It is worth to mention that the content and orientation of the β-phase are the key factors affecting the macroscopic piezoelectric response of PVDF. Thus, we carried out *DSC thermographs* of PVDF NFs arrays to study the thermal behavior of the crystalline polymorph (β- phase). The concerning result is shown in Figure S5. An endothermic peak, corresponding to the melting point (T_m in Figure S5) of the crystalline phase of the PVDF NFs is at 170 ^{o}C. Since PVDF NFs mainly consists of the polar β– phase, this temperature corresponds to the melting point of the polar β– phase. As the polar phase is mainly responsible for the piezoelectric performance of the device, it is expected that the device can be operated within a wide temperature range from room temperature (30 ^{o}C) to 170 ^{o}C.

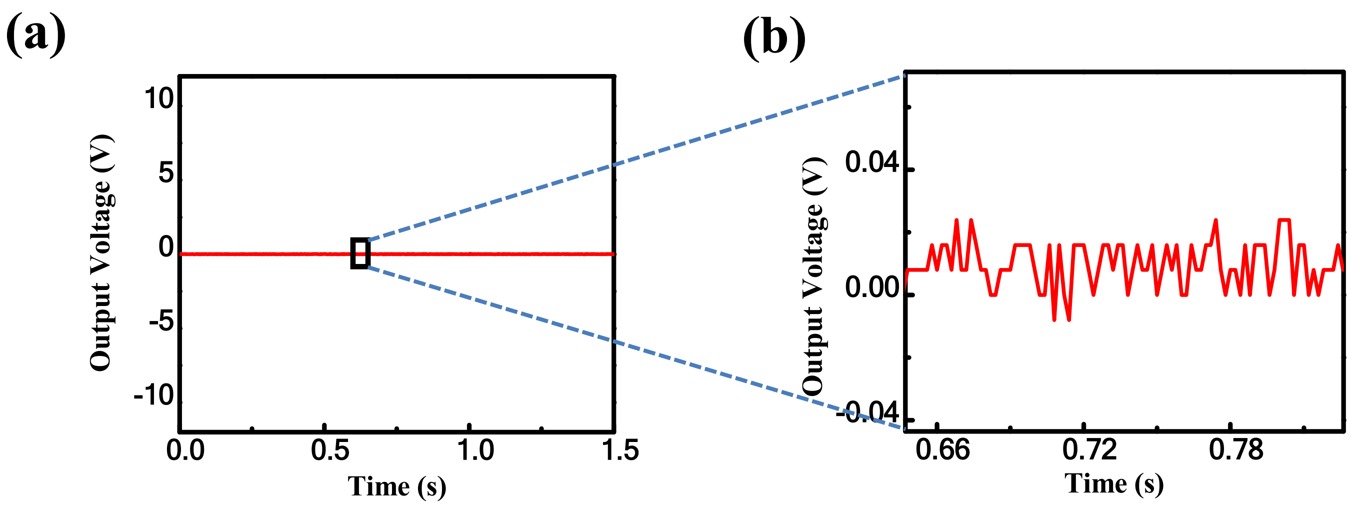

Figure S6. (a) Output voltage from the PDMS based control device (without aligned PVDF arrays and PANI-PVDF NFs mat) with the analogy of POESS under 10 kPa of repeated finger imparting. (b) Enlarged view of the marked region of Figure S6a.

Note S5. Calculation of the piezoelectric coefficient of the POESS.

The charge (Q) generated due to the application of force (F) ~ 8 N in the POESS can be calculated from the following equation by integrating current signal:

$$Q = \int I_{Sc} dt. \tag{5}$$

Q ~ 256 pC was deduced. Subsequently, the magnitude of piezoelectric coefficient can be expressed as,

$$d_{33} = \frac{Q}{F} \tag{6}$$

where we obtained a d_{33} of about 32 pC/N.

Note S6. Calculation of the axial-strain (ε) in the POESS.

The developed axial-strain (ε) in the POESS as a consequence of stress impact is 1.11×10^{-3}, obtained using the equation as $\varepsilon = \sigma_a/Y$, here σ_a is the axial stress (~ 10 kPa) applied upon POESS and Young's modulus is denoted as Y.

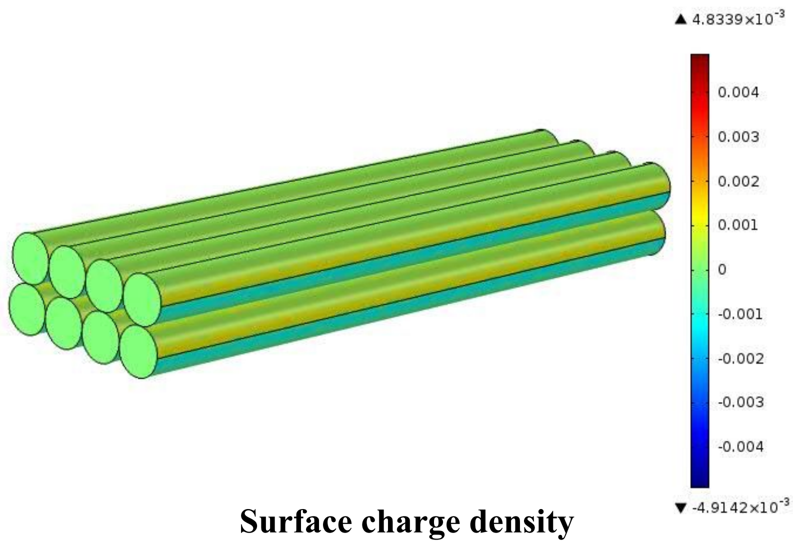

Figure S7: Simulated surface charge density distribution of the POESS under the stress application of 10 kPa.

Note S7. COMSOL simulation.

We used finite-element method (FEM) applying COMSOL Multiphysics software to simulate the deformation and piezo-voltage distribution of the POESS under applied pressure (~ 10 kPa) [S7, S8]. In this study, a standard physical model for piezoelectric simulation in COMSOL software package as commonly used is adopted [S7, S8]. The POESS can be regarded as hundreds of aligned PVDF NFs arrays arranged in parallel fashion. So here we consider a aligned-like structure, mainly presented by PVDF NFs arrays for COMSOL modelling. We want to describe how the electromechanical interaction among nanofibers at micro-scale affects the resulting longitudinal polarization under compressive stress. A 3-dimensional geometry is required for the simulation where a single nanofiber is considered as a cylinder with a diameter of 120 nm which is the average diameter of aligned PVDF NFs. To simplify the simulation, an external boundary load *i.e.*, stress (~ 10 kPa) was applied to the upper surface of the nanofibers, and the other boundaries of the nanofibers were considered as symmetric. In this study, we consider isotropic bulk material properties of the PVDF NFs. The model is meshed with 'physics controlled mesh' and element size 'fine' is used. Due to the direct piezoelectric effect surface displacement of 16 μm under 10 kPa of stress and a potential difference of 26 V were calculated between the top and bottom surface of a single nanofiber. The corresponding voltage distribution and displacement are shown in Figures 5e-5f (main manuscript) and the surface charge density is shown in Figure S7, Supporting Information.

REFERENCES

S1. Zeng, W.; Tao, X.-M.; Chen, S.; Shang, S.; Chanb, H. L. W.; Choyb, S. H. Highly Durable All-fiber Nanogenerator for Mechanical Energy Harvesting. *Energy Environ. Sci.* **2013**, 6, 2631–2638.

S2. Bafqi, M. S. S.; Bagherzadeh, R.; Latifi, M. Fabrication of Composite PVDF-ZnO Nanofiber mats by Electrospinning for Energy Scavenging Application with Enhanced Efficiency. *J Polym Res* **2015**, 22, 130– 139.

S3. Garain, S.; Sinha, T. K.; Adhikary, P.; Henkel, K.; Sen, S.; Ram, S.; Sinha, C.; Schmeiser, D.; Mandal, D. Self-Poled Transparent and Flexible UV Light-Emitting Cerium Complex−PVDF Composite: A High-Performance Nanogenerator. *ACS Appl. Mater. Interfaces* **2015**, 7, 1298−1307.

S4. Maity, K.; Mahanty, B.; Sinha, T. K.; Garain, S.; Biswas, A.; Ghosh, S. K.; Manna, S.; Ray, S. K.; Mandal, D. Two-Dimensional Piezoelectric MoS_2-Modulated Nanogenerator and Nanosensor Made of Poly(vinlydine Fluoride) Nanofiber Webs for Self-Powered Electronics and Robotics. *Energy Technol.* **2017**, *5*, 234 – 243.

S5. Persano, L.; Dagdeviren, C.; Su, Y.; Zhang, Y.; Girardo, S.; Pisignano, D.; Huang, Y.; Rogers, J. A. High Performance Piezoelectric Devices Based on Aligned Arrays of Nanofibers of Poly(vinylidenefluoride-co-trifluoroethylene). *Nat. Commun.* **2013**, 4, 1633 – 1643.

S6. Jin, C. C.; Liu, X. C.; Liu, C. H.; Hwang, H. L.; Wang, Q. Preparation and Structure of Aligned PLZT Nanowires and Their Application in Energy Harvesting. *Applied Surface Science* **2018**, 447, 430–436.

S7. Gui, J.; Zhu, Y.; Zhang, L.; Shu, X.; Liu, W.; Guo, S.; Zhao, X. Enhanced Output-Performance of Piezoelectric Poly(vinylidene fluoride trifluoroethylene) Fibers-based Nanogenerator with Interdigital Electrodes and Well-ordered Cylindrical Cavities. *Appl. Phys. Lett.* **2018**, 112, 072902

S8. Chen, X.; Tian, H.; Li, X.; Shao, J.; Ding, Y.; An, N.; Zhou, Y. A High Performance P(VDF-TrFE) Nanogenerator with Self-Connected and Vertically Integrated Fibers by Patterned EHD Pulling. *Nanoscale* **2015**, 7, 11536–11544.